



Published in final edited form as:

*Biomacromolecules*. 2012 October 8; 13(10): 3343–3354. doi:10.1021/bm301109c.

## Nitric Oxide-Releasing Dendrimers as Antibacterial Agents

Bin Sun, Danielle L. Slomberg, Shalini L. Chudasama, Yuan Lu, and Mark H. Schoenfisch

Department of Chemistry, University of North Carolina at Chapel Hill, Chapel Hill, NC 27599

### Abstract

The antibacterial activity of a series of nitric oxide (NO)-releasing poly(propylene imine) (PPI) dendrimers was evaluated against both Gram-positive and Gram-negative pathogenic bacteria, including methicillin-resistant *Staphylococcus aureus*. A direct comparison of the bactericidal efficacy between NO-releasing and control PPI dendrimers (i.e., non-NO-releasing) revealed both enhanced biocidal action of NO-releasing dendrimers and reduced toxicity against mammalian fibroblast cells. Antibacterial activity for the NO donor-functionalized PPI dendrimers was shown to be a function of both dendrimer size (molecular weight) and exterior functionality. In addition to minimal toxicity against fibroblasts, NO-releasing PPI dendrimers modified with styrene oxide exhibited the greatest biocidal activity (9.999% killing) against all bacterial strains tested. The *N*-diazoniumdiolate NO donor-functionalized PPI dendrimers presented in this study hold promise as effective NO-based therapeutics for combating bacterial infections.

### Introduction

Bacterial infections in general pose tremendous challenges to human health in community and nosocomial settings, particularly those originating from antibiotic-resistant strains.<sup>1–3</sup> Dendrimers are a family of macromolecular scaffolds with hyper-branched architectures and multivalent surfaces<sup>4–12</sup> that have been used for a broad range of biomedical applications including drug delivery,<sup>13–21</sup> gene transfection,<sup>22–27</sup> and tissue engineering.<sup>28–31</sup> Examples of dendritic scaffolds used for biomedical applications include poly(propylene imine) (PPI), polyamidoamine (PAMAM), poly(L-lysine) (PLL), polyesters, and poly(2,2-bis(hydroxymethyl)propionic acid).<sup>6</sup> Recent research has highlighted the versatility of dendrimer synthesis to create antibacterial dendritic scaffolds of unique size and surface functionality.<sup>14–17,32</sup> For example, Cooper and coworkers synthesized quaternary ammonium-functionalized poly(propylene imine) (PPI) dendrimers and demonstrated their antimicrobial activity as a function of dendrimer size and quaternary ammonium structure.<sup>15</sup> Despite promising biocidal activity, the cationic dendrimers were inherently toxic to mammalian cells. In an effort to design less toxic constructs, Cai and coworkers partially modified the exterior of primary amine-functionalized polyamidoamine dendrimers (PAMAM-NH<sub>2</sub>) with poly(ethylene glycol) (PEG) to mask the peripheral cationic charge.<sup>14,17</sup> The resulting PEG-modified PAMAM conjugates exhibited reduced toxicity to human corneal epithelial cells, while maintaining their antibacterial efficacy against several bacterial species. Anionic amphiphilic dendrimers have also been shown to selectively kill Gram-positive *Bacillus subtilis* with minimal toxicity to human umbilical vein endothelial cells (HUVECs).<sup>16</sup>

Correspondence to: Mark H. Schoenfisch.

Supporting Information Confocal negative controls of *P. aeruginosa* cells in the presence of DAF-2 and PI alone (Figure S1). This material is available free of charge via the Internet at <http://pubs.acs.org>.

Nitric oxide (NO), a phagocyte-derived, reactive free radical plays key roles in the host defense against microbial pathogens.<sup>33–36</sup> Broad-spectrum antibacterial activity results from reactive byproducts of NO (e.g., peroxynitrite and dinitrogen trioxide) that negatively impact the integrity of the bacteria membrane and cell function via oxidative and nitrosative stress. The design of NO-based macromolecules thus represents an active area of research in the development of next generation antibacterial agents and other therapeutics.<sup>37–41</sup> For example, our group has prepared a number of macromolecular NO donors including gold clusters,<sup>42,43</sup> dendrimers,<sup>44–46</sup> and silica-based nanoparticles<sup>47–51</sup> to facilitate improved storage and delivery for therapeutic applications. Hetrick et al. first reported on the enhanced antibacterial properties of macromolecular-derived NO compared to small molecule NO donors.<sup>52</sup> In subsequent work, Carpenter et al. described the importance of particle size on biocidal activity against Gram-negative *Pseudomonas aeruginosa*.<sup>50</sup> Collectively, this earlier work illustrates the advantage of killing microbial pathogens with macromolecular NO donors.

To further diversify the available macromolecular NO donor vehicles, we reported the synthesis of structurally diverse *N*-diazoniumdiolate-functionalized poly(propylene imine) (PPI) dendrimers capable of tunable NO storage and release (0.9–3.8  $\mu\text{mol NO}\cdot\text{mg}^{-1}$  totals and 0.3 to 4.9 h half-lives).<sup>44,46</sup> However, an evaluation of the bactericidal activity of these structurally diverse NO-releasing PPI dendrimers was not carried out. We hypothesize that both the size and exterior functionality may enable tuning of both the biocidal activity and cytotoxicity for antibacterial applications.

## Methods

### Materials

Propylene oxide (PO), styrene oxide (SO), poly(ethylene glycol) methyl ether acrylate (average  $M_n = 480$ ) (PEG), and propidium iodide (PI) were purchased from Sigma-Aldrich (St. Louis, MO). Sodium methoxide (5.4 M solution in methanol) was obtained from Acros Organics Geel, Belgium). Common laboratory salts and solvents were purchased from Fisher Scientific (Pittsburgh, PA). Unless noted otherwise, these and other materials were used as received without further purification. Tryptic soy broth (TSB) and tryptic soy agar (TSA) were obtained from Becton, Dickinson and Company (Franklin Lakes, NJ). Rhodamine B isothiocyanate (RITC) was purchased from Aldrich Chemical Co. (Milwaukee, WI). Spectra/Por Float-A-Lyzers for dialysis of the dendrimers were purchased from Spectrum Laboratories, Inc. (Rancho Dominguez, CA). 4,5-Diaminofluorescein diacetate (DAF-2 DA) was purchased from Calbiochem (San Diego, CA). Glass bottom microscopy dishes were received from MatTek Corporation (Ashland, MA).

### Synthesis of Secondary Amine- and Diazoniumdiolate-Functionalized PPI Dendrimers

Secondary amine-functionalized PPI dendrimers (G2 and G5) were synthesized as described previously.<sup>44,46</sup> Briefly, 100 mg primary amine-functionalized G2-PPI dendrimer **7** (G2-PPI-NH<sub>2</sub>) was dissolved in methanol (2 mL). One molar equivalent of PO, SO, or PEG was then added to the G2-PPI-NH<sub>2</sub> solution (methanol) with constant stirring at room temperature for 4 d to yield the secondary amine-functionalized G2-PPI conjugates (i.e., G2-PPI-PO **1**, G2-PPI-PEG **3**, G2-PPI-SO **5**). Likewise, secondary amine-functionalized G5-PPI conjugates (i.e., G5-PPI-PO **2**, G5-PPI-PEG **4**, G5-PPI-SO **6**) were formed via the reactions of G5-PPI-NH<sub>2</sub> **8** with PO, PEG, and SO, respectively. Solvent was then removed under reduced pressure. Dendrimers **1–6** were dissolved in water followed by dialysis against water and lyophilization. The resulting secondary amine-functionalized dendrimers **1–6** (Figure 1) were characterized by <sup>1</sup>H and <sup>13</sup>C nuclear magnetic resonance (NMR) spectroscopy using Bruker (400 MHz) and Varian (600 MHz) spectrometers.

Representative  $^1\text{H}$  and  $^{13}\text{C}$  NMR data of secondary amine-functionalized G5-PPI conjugates formed via the reactions of G5-PPI-NH<sub>2</sub> **8** with PO, PEG, and SO (G5-PPI-PO **2**, G5-PPI-PEG **4**, G5-PPI-SO **6**) are as follows: G5-PPI-PO **2**:  $^1\text{H}$  NMR (400 MHz, CD<sub>3</sub>OD,  $\delta$ ): 3.70 (CH<sub>2</sub>CH(OH)CH<sub>3</sub>), 2.60–2.62 (CH<sub>2</sub>CH(OH)CH<sub>3</sub>, NCH<sub>2</sub>CH<sub>2</sub>CH<sub>2</sub>NH), 2.40 (NCH<sub>2</sub>CH<sub>2</sub>CH<sub>2</sub>NH), 1.60 (NCH<sub>2</sub>CH<sub>2</sub>CH<sub>2</sub>NH), 1.00 (CH<sub>2</sub>CH(OH)CH<sub>3</sub>).  $^{13}\text{C}$  NMR (400 MHz, CD<sub>3</sub>OD,  $\delta$ ): 66.9, 58.2, 53.7, 52.8, 41.2, 30.8, 27.6, 24.9, 21.8. G5-PPI-PEG **4**:  $^1\text{H}$  NMR (400 MHz, CD<sub>3</sub>OD,  $\delta$ ): 2.60 (NCH<sub>2</sub>CH<sub>2</sub>CH<sub>2</sub>NH), 2.40 (NCH<sub>2</sub>CH<sub>2</sub>CH<sub>2</sub>NH), 1.60 (NCH<sub>2</sub>CH<sub>2</sub>CH<sub>2</sub>NH), 3.40–3.70 (OCH<sub>2</sub>CH<sub>2</sub>O), 2.80 (CH<sub>2</sub>NHCH<sub>2</sub>CHCOOPEG), 2.65 (CH<sub>2</sub>NHCH<sub>2</sub>CHCOOPEG), 2.42 (CH<sub>2</sub>NHCH<sub>2</sub>CHCOOPEG).  $^{13}\text{C}$  NMR (400 MHz, CD<sub>3</sub>OD,  $\delta$ ): 172, 71.6, 70.85, 69.3, 60.1, 57.0, 51.4, 43.9, 39.1, 22.9. G5-PPI-SO **6**:  $^1\text{H}$  NMR (400 MHz, CD<sub>3</sub>OD,  $\delta$ ): 7.50–7.20 (CH<sub>2</sub>CH(OH)Ph), 3.70 (CH<sub>2</sub>CH(OH)Ph), 2.72 (CH<sub>2</sub>CH(OH)Ph), 2.60 (NCH<sub>2</sub>CH<sub>2</sub>CH<sub>2</sub>NH), 2.40 (NCH<sub>2</sub>CH<sub>2</sub>CH<sub>2</sub>NH), 1.60 (NCH<sub>2</sub>CH<sub>2</sub>CH<sub>2</sub>NH).  $^{13}\text{C}$  NMR (400 MHz, CD<sub>3</sub>OD,  $\delta$ ): 140.6, 128.2, 127.5, 127.3, 125.8, 71.9, 57.1, 52.4, 45.6, 39.8, 26.3, 23.6.

For the synthesis of *N*-diazoniumdiolate-functionalized PPI dendrimers **1a–6a**, one equivalent of 5.4 M sodium methoxide solution in methanol (with respect to the molar amount of primary amine functionalities in PPI-NH<sub>2</sub> used to synthesize dendrimers **1–6**) was added to a vial containing dendrimers **1–6** in methanol (2 mL). After placing the vial in a stainless steel reactor, the headspace was flushed with argon three times followed by three longer purges with argon (3 × 10 min) to remove oxygen from the stirred solution. The reactor was then filled with NO (10 atm) (purified over KOH pellets for 30 min to remove trace NO degradation products) at ambient temperature. After 3 d, the NO was expunged using the same argon flushing procedure described above to remove unreacted NO from the reaction solution. The formation of the *N*-diazoniumdiolate functionality was confirmed by UV-vis spectroscopy (Perkin-Elmer Lambda 40 spectrophotometer (Norwalk, CT)) with the presence of a strong absorbance peak at ~250 nm (solution in methanol). Zeta potential of the dendrimers was determined using a Zetasizer Nano ZS Zeta Potential Instrument (Malvern, UK). Samples (~2 mg·mL<sup>-1</sup>) were prepared in phosphate buffer (10 mM, pH = 7.4) and immediately injected into a folded capillary cell for zeta-potential analysis.<sup>50</sup>

### Characterization of NO Storage and Release

Nitric oxide release was measured using a Sievers 280i Chemiluminescence Nitric Oxide Analyzer (Boulder, CO). Chemiluminescence was the chosen measurement technique as it measures NO levels directly and minimizes side reactions that can occur prior to analysis.<sup>40,53</sup> The NO analyzer was calibrated using an atmospheric (blank) sample passed through an NO zero filter and a 26.8 ppm NO standard. Aliquots (~10–25  $\mu\text{L}$ ) of *N*-diazoniumdiolate-functionalized PPI **1a–6a** as a solution in methanol (~7–200 mM) were added to 30 mL phosphate buffered saline (PBS) (10 mM, pH = 7.4) at 37 °C to initiate NO release. The analysis was terminated when the NO release fell below 10 ppb NO·mg<sup>-1</sup> dendrimer. Chemiluminescence data for the NO-releasing dendrimers were represented as: i) total amount of NO release (t[NO],  $\mu\text{mol NO}\cdot\text{mg}^{-1}$ , and  $\mu\text{mol NO}\cdot\mu\text{mol}^{-1}$  of secondary amine-functionalized dendrimers); ii) amount of NO released over the 2 h time course of the bactericidal assays (t[NO]<sub>2h</sub>,  $\mu\text{mol NO}\cdot\text{mg}^{-1}$ , and  $\mu\text{mol NO}\cdot\mu\text{mol}^{-1}$  of secondary amine-functionalized dendrimers); iii) maximum flux of NO release ([NO]<sub>max</sub>, ppb·mg<sup>-1</sup>, and ppb· $\mu\text{mol}^{-1}$  of secondary aminefunctionalized dendrimers); iv) time required to reach [NO]<sub>max</sub> (t<sub>m</sub>); v) half-life (t<sub>1/2</sub>) of NO release; and, vi) conversion efficiency defined as percentages of amine functionalities in PPI conjugates **1–6** converted to *N*-diazoniumdiolate functionality (i.e., total moles of NO release divided by twice the molar amount of primary amine functionalities in G2 and G5 PPI-NH<sub>2</sub> used to initially synthesize secondary amine-functionalized dendrimer conjugates).

## Bacterial Culture

The bacterial strains used in this study were obtained from American Type Culture Collection (ATCC; Manassas, VA) and included *Pseudomonas aeruginosa* (19143), standard *Staphylococcus aureus* (29213), and methicillin-resistant *S. aureus* (MRSA) (33591). Lyophilized bacteria were reconstituted in TSB and cultured overnight at 37 °C. A 0.5 mL aliquot of culture was grown in 50 mL of TSB for 2–4 h until reaching an optical density at 600 nm (OD<sub>600</sub>) of 0.1–0.5. The resulting culture was pelleted by centrifugation, resuspended in 15% glycerol (v/v in PBS), and stored at –80 °C in 1 mL aliquots. For daily experiments, colonies of bacteria culture were inoculated in 2 mL of TSB overnight at 37 °C and recultured in fresh TSB the next day. The bacteria were then grown to mid-exponential phase (~1 × 10<sup>8</sup> colony forming units (cfu)·mL<sup>-1</sup>) as determined by OD<sub>600</sub> measurements. The relationship between the OD<sub>600</sub> and the concentration of bacteria in the culture suspension was calibrated for each strain using a Spectronic 301 spectrophotometer (Milton Roy; Ivyland, PA) and enumeration of colony forming units from culture dilutions grown on TSA plates. The resulting 1 × 10<sup>8</sup> cfu·mL<sup>-1</sup> bacterial suspension in TSB was centrifuged for 15 min at 3645 × *g*, followed by decanting of the supernatant. The pellet of bacterial cells was resuspended in PBS and adjusted to an appropriate concentration in PBS.

## Bactericidal Assays

The minimum bactericidal concentration (MBC) was determined as the concentration of dendrimers that resulted in either a 3 or 5 log reduction in viability compared to untreated cells for a particular bacterial strain after 2 h. Each strain of bacteria was tested in triplicate over an optimized concentration range. To evaluate the bactericidal efficacy of primary and secondary amine-functionalized dendrimers **1–8**, solutions of dendrimers in PBS (10 mM, pH = 7.4) or acetate buffer (20 mM, pH = 5.0, for dendrimers **5** and **6** to increase long-term solubility) were prepared and added to an appropriate volume of bacterial suspension in PBS for a final starting inoculum concentration of 1 × 10<sup>6</sup> cfu·mL<sup>-1</sup>. To test the bactericidal properties of NO-releasing dendrimers **1a–6a**, an appropriate volume of dendrimer solution in methanol was premeasured into a glass vial and dried under vacuum for 2 h. The necessary volume of 1 × 10<sup>6</sup> or 1 × 10<sup>7</sup> cfu·mL<sup>-1</sup> bacterial suspension (3 and 5 log reduction testing, respectively) was then added to obtain the target dendrimer concentration. The starting inoculum concentration (1 × 10<sup>6</sup> or 1 × 10<sup>7</sup> cfu·mL<sup>-1</sup>) for 3 or 5 log reduction testing was selected on the basis of the limit of detection for plating (2.5 × 10<sup>3</sup> cfu·mL<sup>-1</sup>).<sup>54</sup> After 2 h of incubation at 37 °C, bacterial culture dilutions were prepared in PBS. A predetermined aliquot (100 μL) of each dilution was plated onto TSA plates and incubated at 37 °C overnight. The number of colonies was enumerated to determine cell viability at the time of plating.

## Confocal Microscopy for Detection of Intracellular NO and Cell Death

*N*-diazoniumdiolate-modified *N*-(6-aminohexyl) aminopropyltrimethoxysilane (AHAP3)/tetraethoxysilane (TEOS) silica nanoparticles (50 nm) were synthesized as described previously.<sup>50</sup> *P. aeruginosa* was cultured in TSB to a concentration of 1 × 10<sup>8</sup> cfu·mL<sup>-1</sup>, collected via centrifugation (3645 × *g* for 10 min), resuspended in sterile PBS, and adjusted to 1 × 10<sup>6</sup> cfu·mL<sup>-1</sup> in PBS supplemented with 10 μM DAF-2 DA and 30 μM PI. Aliquots of the bacteria solution were incubated in a glass bottom confocal dish for 45 min at 37 °C. A Zeiss 510 Meta inverted laser scanning confocal microscope with a 488 nm Ar excitation laser (2.0% intensity) and a BP 505–530 nm filter was used to obtain DAF-2 (green) fluorescence images. A 543 nm HeNe excitation laser (25.3% intensity) with a BP 560–615 nm filter was used to obtain PI (red) fluorescence images. The bright field and fluorescence images were collected using a N.A. 1.2 C-apochromat water immersion lens with a 40× objective. Suspensions (1.5 mL) of G2 (17.4 μg·mL<sup>-1</sup>) or G5 (20.0 μg·mL<sup>-1</sup>) PPI-SO NO-

releasing dendrimers or 50 nm NO-releasing AHAP3/TEOS nanoparticles ( $44.0 \mu\text{g}\cdot\text{mL}^{-1}$ ) in PBS supplemented with  $10 \mu\text{M}$  DAF-2 DA and  $30 \mu\text{M}$  PI were added to the bacteria solution (1.5 mL) in the glass confocal dish. Images were collected every 2 min to observe intracellular NO concentrations and bacteria cell death temporally.

### Confocal Microscopy for Association of Dendrimers with Bacteria Cells

The synthesis of fluorescently labeled control or NO-releasing G2-PPI-PO dendrimers was adapted from a previously reported literature procedure.<sup>50</sup> Briefly, G2-PPI-NH<sub>2</sub> (100 mg) and rhodamine B isothiocyanate (RITC) (7.5 mg, 14.0 mmol) were dissolved in methanol (2 mL). The solution was stirred for 24 h in the dark. The product solution was concentrated under reduced pressure, dissolved in water (~3 mL), and added to a Spectra/Por Float-A-Lyzer (5 mL, 1000 MWCO) for dialysis in 0.1 M NaCl (2 L) for 24 h, followed by dialysis in ultrapure Milli-Q water for 3 d ( $3 \times 2$  L). The aqueous sample was frozen and lyophilized to yield RITC-labeled G2-PPI-NH<sub>2</sub>. Next, fluorescently labeled G2-PPI-NH<sub>2</sub> was modified with one molar equivalent of PO alone and/or further reacted with high-pressure NO under basic conditions as described above to yield RITC-labeled control and NO-releasing G2-PPI-PO dendrimers. *S. aureus* was cultured in TSB to a concentration of  $1 \times 10^8$  cfu·mL<sup>-1</sup>, collected *via* centrifugation ( $3645 \times g$  for 10 min), resuspended in sterile PBS, and adjusted to  $1 \times 10^6$  cfu·mL<sup>-1</sup>. Aliquots of the bacteria solution were incubated in a glass bottom confocal dish for 45 min at 37 °C. A Zeiss 510 Meta inverted laser scanning confocal microscope with a 543 nm HeNe excitation laser (80% intensity) and a LP 585 nm filter was used to obtain fluorescence images of the RITC-modified dendrimers. The bright field and fluorescence images were collected using a N.A. 1.2 C-apochromat water immersion lens with a 40× objective. Solutions of RITC-labeled control ( $400 \mu\text{g}\cdot\text{mL}^{-1}$ ) or NO-releasing G2 ( $400 \mu\text{g}\cdot\text{mL}^{-1}$ ) PPI-PO dendrimers in PBS (1.5 mL) were added to the bacteria solution (1.5 mL) in the glass confocal dish to achieve a final concentration of  $200 \mu\text{g}\cdot\text{mL}^{-1}$ . Images were collected every 2 min to monitor association of the dendrimers with *S. aureus* temporally.

### In Vitro MTS Cell Proliferation Assay

Mouse fibroblast cells (L929) were purchased from American Type Culture Collection (ATCC; Manassas, VA). Initial seeding densities of  $30,000$  cells·mL<sup>-1</sup> in 200  $\mu\text{L}$  of growth medium (Dulbecco's modified Eagle's medium (DMEM), 10% fetal bovine serum (FBS), penicillin  $100$  units·mL<sup>-1</sup>, and streptomycin  $100 \mu\text{g}\cdot\text{mL}^{-1}$ ) were used in clear 96-well culture plates. After plating, all cells were incubated at 37 °C for 48 h with toxicity experiments carried out at ~80% confluence. Dendrimer solutions (50  $\mu\text{L}$ ) in chilled 4-(2-hydroxyethyl)-1-piperazineethanesulfonic acid buffer (HEPES; 20 mM, pH = 7.4) or acetate buffer (20 mM, pH = 5.0, for dendrimers **5** and **6**) were prepared in triplicate at desired concentrations and added to cells immediately after an initial replacement of growth media with fresh media (200  $\mu\text{L}$ ). Cells were incubated with dendrimers for 4 h before aspirating the media from all samples. Fresh media (100  $\mu\text{L}$ ) was added to the cells along with 20  $\mu\text{L}$  of the MTS assay reagent (CellTiter 96 Aqueous Non-Radioactive Cell Proliferation Assay, Promega, Madison, WI). The mitogenic MTS assay for cell viability relies upon the reduction of a yellow MTS compound (3-(4,5-dimethylthiazol-2-yl)-5-(3-carboxymethoxyphenyl)-2-(4-sulfophenyl)-2H-tetrazolium) due to mitochondrial respiration. The reduction to a purple formazan derivative occurs only in viable cells. The absorbance of this colored solution was quantified at 490 nm using a Labsystems Multiskan RC microplate spectrophotometer (Helsinki, Finland). Untreated cells were used as controls. Results were expressed as percentage of relative cell viability =  $[(\text{Abs}_{490}$  of dendrimer treated cells -  $\text{Abs}_{490}$  of blank)/( $\text{Abs}_{490}$  of untreated cells -  $\text{Abs}_{490}$  of blank)]  $\times$  100%.

## Results and Discussion

### Characterization of Nitric Oxide Release from Dendrimer-Bound *N*-Diazeniumdiolates

Recent research suggests that both the size and exterior functionality of dendrimer scaffolds may play important roles in their antibacterial activity.<sup>14–17</sup> As such, we synthesized NO-releasing PPI dendrimers of distinct size and exterior properties (e.g., aromatic, hydrophilic, hydrophobic) to design antibacterial scaffolds with minimal toxicity to healthy cells (Figure 1).<sup>44,46</sup>

Briefly, the dendrimer exterior of G2 or G5 PPI-NH<sub>2</sub> was modified with PO or SO via a ring opening reaction or PEG via conjugate addition to yield secondary amine-functionalized dendrimers **1–6**. The use of epoxides and acrylates for dendrimer modification allows for the tailoring of the exterior functionality with respect to steric environment, hydrophobicity, and biocompatibility. Subsequent reaction of accessible secondary amines with high-pressure NO under basic conditions resulted in the formation of *N*-diazeniumdiolate-functionalized dendritic scaffolds **1a–6a** with suitable amine-to-diazeniumdiolate conversion efficiencies (~19–35%) and NO payloads (~1.1–3.8 μmol·mg<sup>-1</sup>) (Table 1). The practical advantage of this synthetic approach is that it allows for i) the direct comparison of antimicrobial properties of NO-releasing dendrimers with secondary amine-functionalized control dendrimers (i.e., non-NO-releasing); and, ii) the identification of structural motifs at the dendrimer exterior that may influence the bactericidal efficacy of these materials. As determined using chemiluminescence, the NO-release kinetics from these macromolecular NO-donor scaffolds were similar regardless of size or exterior modification, with NO release half-lives (*t*<sub>1/2</sub>) ranging from ~0.7–1.7 h and the time required to reach the maximum NO flux (*t*<sub>m</sub>) from ~1.5–3 min (Table 1). To understand the influence of *N*-diazeniumdiolate conversion on the dendrimer surface charge, the zeta potentials of control and NO-releasing dendrimers in phosphate buffer (10 mM, pH = 7.4) were quantified (Table 2). As expected, control dendrimers **1–6** exhibited positive zeta potentials (~+7–26 mV) due to the protonation of exterior secondary amines at pH 7.4. Less positive and even negative zeta potentials (~–14 to +13 mV; listed in bold) were measured for NO-releasing dendritic scaffolds **1a–6a** since the amines were functionalized with *N*-diazeniumdiolate NO donors.

Multivalent dendrimer-bound NO donors with 8 and 64 terminal functional groups (G2 and G5) were employed to understand the influence of dendrimer size on bactericidal efficacy. To compare the localized concentration of NO delivered into solution from a single dendritic scaffold of two different sizes, the maximum NO flux ([NO]<sub>m</sub>, ppb) and the amount of NO generated (t[NO]<sub>2h</sub>, μmol) during 2 h bactericidal assays were determined on a per micromole basis. As shown in Table 1, the larger dendritic scaffolds exhibited markedly greater NO flux (~4–6 folds) and release levels (~8–10×) over 2 h (noted in bold) than their smaller analogues. This data reveals the ability of NO-releasing PPI dendrimers to deliver large localized doses of NO as a function of dendrimer size, a potential benefit for fine-tuning antimicrobial activity.

### Broad-Spectrum Bactericidal Efficacy of NO-Releasing Dendrimers

Gram-negative (*P. aeruginosa*), Gram-positive (*S. aureus*), and antibiotic-resistant species (MRSA) were exposed to control **1–6** and NO-releasing dendrimers **1a–6a** to evaluate the ability of dendrimers to kill bacteria. Bacterial viability assays were performed under static conditions to determine the lowest dendrimer concentration (MBC) required to elicit a 3-log reduction. Although methanol (used as a solvent in the dendrimer synthesis) was removed thoroughly under reduced pressure and lyophilization, the toxicity of methanol to both Gram-negative *P. aeruginosa* and Gram-positive *S. aureus* was also evaluated to ensure that any residual methanol did not influence MBC values. No methanol toxicity up to 5000 μM

methanol (e.g., markedly greater than the dendrimer concentrations used in this study) was observed over the 2-h time course of the bactericidal assay.

The amount of NO delivered over 2 h from dendrimers **1a–6a** ( $t[\text{NO}]_{2\text{h}}$ ,  $\mu\text{mol NO}\cdot\mu\text{mol}^{-1}$  of dendrimers; Table 1) was also employed to quantitatively assess the NO dose necessary to achieve 99.9% bacterial killing. Figure 2 illustrates the dose-dependent bactericidal activity for both control and NO-releasing dendrimers against Gram-negative *P. aeruginosa*. The corresponding NO release at specific concentrations of NO-releasing dendrimers ( $\mu\text{mol NO}\cdot\text{L}^{-1}$ ) was derived by multiplying  $t[\text{NO}]_{2\text{h}}$  ( $\mu\text{mol NO}\cdot\mu\text{mol}^{-1}$  of dendrimers; Table 1) with the concentrations of the dendrimers ( $\mu\text{M}$ ). The MBCs and the bactericidal NO doses required for these dendrimers are provided in Table 3 (i.e., the bactericidal NO dose ( $\mu\text{mol NO}\cdot\text{L}^{-1}$ ) =  $t[\text{NO}]_{2\text{h}}$  ( $\mu\text{mol NO}\cdot\mu\text{mol}^{-1}$  of dendrimers; Table 1)  $\times$  MBC ( $\mu\text{M}$ )). In general, the concentration of NO-releasing dendrimers **1a–6a** required to eradicate (completely kill) *P. aeruginosa* was substantially lower than that of control dendrimers **1–6**, indicating enhanced bactericidal action exerted by NO. This increase in bactericidal efficacy may be attributed to both oxidative and nitrosative stresses on the bacteria, driven by reactive NO byproducts such as dinitrogen trioxide ( $\text{N}_2\text{O}_3$ ) and peroxynitrite ( $\text{ONOO}^-$ ).<sup>33,34,52,55</sup> While oxidative stress leads to membrane destruction via peroxynitrite-induced lipid peroxidation, nitrosative stress (exerted by reactive byproducts such as  $\text{N}_2\text{O}_3$ ) may result in protein S-nitrosation and DNA deamination, also disrupting microbial viability. As expected, the NO poses a biocidal action on the bacteria.

Further inspection of these data reveals that the bactericidal concentrations for both NO-releasing and control dendrimers (G2 or G5) varied substantially as a function of their exterior functionality. For example, both NO-releasing and control G2-PPI-SO dendrimers (**5a** and **5**) exhibited the greatest bactericidal efficacy against *P. aeruginosa* as evidenced by the lowest concentration of dendrimers required for complete killing (1.0 and 5.0  $\mu\text{M}$ , respectively). As shown in Figure 2A, intermediate efficacy was observed for the NO-releasing and control G2-PO-modified PPI conjugates (**1a** and **1**) (300 and 400  $\mu\text{M}$ , respectively). The G2-PEG-modified scaffolds (**3a** and **3**) were least effective, requiring the largest dendrimer concentrations for *P. aeruginosa* killing (320 and 4800  $\mu\text{M}$  for NO-releasing and control scaffolds, respectively) (Figure 2C). Similar trends were observed for the larger (G5) NO-releasing and control dendrimers (Figures 2B, D, F).

Cooper and coworkers have attributed the bactericidal action of cationic dendritic scaffolds to the disruption of the cytoplasmic membrane of the bacteria, initially by dendrimer association with the bacterial outer surface and then dendrimer penetration through the cell walls.<sup>15,56</sup> The mechanism by which this initial association occurs is largely dependent on electrostatic and hydrophobic interactions between the cationic dendrimers and the negatively-charged outer membrane of the bacteria. As such, the low bactericidal activity observed for PEG-modified dendrimers is the result of decreased electrostatic interactions between the dendrimer scaffold and the bacteria since the exterior PEG groups greatly reduce the positive surface charge of the scaffold. As indicated by a more positive zeta potential (Table 2), we hypothesize that the enhanced bactericidal activity of the SO-modified dendrimers is the result of increased electrostatic interactions between the dendrimers and bacteria, and thus more effective (i.e., localized) NO release. Others have reported that the balance between hydrophilic and lipophilic regions within their chemical structures influences the antimicrobial properties of cationic dendrimers.<sup>14,15</sup> Indeed, the improved bacteria killing observed for SO-modified dendrimers may be attributed, at least partially, to the increased exterior hydrophobicity compared to PO- or PEG-modified dendrimers. In addition to cytoplasmic membrane disruption, Lucchini et al. reported that small molecule benzyl and phenethyl alcohols greatly influenced protein synthesis related to protein function.<sup>57</sup> Thus, the enhanced efficacy of the SO-modified dendrimers may also

result from the multivalent benzyl alcohol-like moieties altering bacteria protein synthesis. Of note, confirming such mechanism is beyond the scope of this work.

As shown in Table 3, the NO dosage necessary for complete bacterial killing over 2 h was significantly lower for the larger dendrimers (e.g., 284 vs 897  $\mu\text{mol NO}\cdot\text{L}^{-1}$  for G5 and G2 PPI-PO **2a** and **1a**, respectively). The greater efficacy observed for the larger scaffolds results from the increased density of *N*-diazoniumdiolate functionalities, enabling greater localized NO delivery in close proximity to the bacterial cells. Although noted for both PPI-PO and PPI-PEG analogues, the NO dose required for G5 PPI-SO **6a** to kill *P. aeruginosa* (7.6  $\mu\text{mol NO}\cdot\text{L}^{-1}$ ) was greater than that required from the corresponding smaller analogue **5a** (2.0  $\mu\text{mol NO}\cdot\text{L}^{-1}$ ). The enhanced efficacy for the G2 PPI-SO **6a** may result from faster diffusion of the smaller aromatic-modified scaffold into/across the bacterial cell walls despite lower NO donor density. In addition, the amount of NO required for complete bacterial killing (3-log reduction for *P. aeruginosa*) is significantly less for both G2 and G5-SO-modified dendrimers (2.0 and 7.6  $\mu\text{mol NO}\cdot\text{L}^{-1}$ , respectively) compared to previously reported 50 nm AHAP3/TEOS nanoparticles (376  $\mu\text{mol NO}\cdot\text{L}^{-1}$ ).<sup>50</sup>

To confirm whether the enhanced bactericidal efficacy of the smaller NO-releasing G2- PPI-SO **5a** was due to faster scaffold diffusion into *P. aeruginosa* cells, and thus enhanced efficiency of NO delivery, intracellular NO concentrations were visualized temporally using confocal microscopy and an NO sensitive dye, 4,5-diaminofluorescein diacetate (DAF-2 DA). Briefly, DAF-2 DA is membrane-permeable until hydrolyzed internally by intracellular esterases to an impermeable form, 4,5-diaminofluorescein (DAF-2).<sup>52</sup> In the presence of oxygen and NO, DAF-2 is converted to a green fluorescent derivative, triazolofluorescein. Bacteria were also imaged in the presence of propidium iodide (PI), a dye that permeates compromised cell membranes.<sup>52</sup> After PI passes through the cell membrane, it binds nucleic acid material, resulting in red fluorescence. In this regard, PI entering the cell indicates a compromised membrane and cell death. In the absence of the NO-releasing scaffolds, the cells were imaged with both DAF-2 DA and PI using identical laser settings; dendrimer autofluorescence was not observed throughout the time course of the experiment (see Figure S1; Supporting Information). These results served as negative controls for the study.

The NO-releasing dendrimers were introduced to the suspension of *P. aeruginosa* cells at an NO dosage of 10  $\mu\text{mol}\cdot\text{L}^{-1}$ . As expected, the DAF-2 signal for the faster diffusing, G2-PPI-SO **5a** appeared first at 46 min, followed by the appearance of the DAF-2 signal for the G5-PPI-SO dendrimer **6a** at 60 min (Figure 3). Indeed, the smaller G2 **5a** dendrimers resulted in more efficient NO delivery to the bacterium. To facilitate comparison of NO delivery from the dendrimers with silica scaffolds, we also exposed the *P. aeruginosa* cells to 50 nm AHAP3/TEOS silica nanoparticles at a similar NO dosage (10  $\mu\text{mol}\cdot\text{L}^{-1}$ ).<sup>50</sup> Green fluorescence was observed at 60 min for the 50 nm AHAP3/TEOS silica particles, signaling an increase in intracellular NO. However, the fluorescence intensity was always less than that observed for the dendrimers throughout the time course of the experiment indicating less efficient NO delivery to the interior of the bacteria relative to the dendrimer scaffolds.

In addition to intracellular NO visualization, we also observed red fluorescence (from PI) for *P. aeruginosa* cells with compromised membranes. For the NO-releasing G2-PPI-SO dendrimer **5a**, red fluorescence was observed after 64 min. Red fluorescence (PI signal) for the slower diffusing NO-releasing G5-PPI-SO dendrimer **6a** appeared at 94 min. Of note, PI signal was not visualized in *P. aeruginosa* cells after exposure to the NO-releasing 50 nm AHAP/TEOS particles at 94 min. We hypothesize that the larger silica scaffold was unable to deliver NO to the bacteria cells at concentrations necessary to compromise the membrane and allow for PI penetration. In contrast, the dendritic scaffold facilitated more efficient NO



delivery to and across the cell surface (membrane), resulting in enhanced bactericidal efficacy.

The bactericidal efficacy of the dendrimers was also assessed using Gram-positive *S. aureus*. As expected based on NO's broad-spectrum activity,<sup>33</sup> the NO-releasing dendritic scaffolds also exhibited greater bactericidal efficacy against *S. aureus* compared to control dendrimers (Figure 4 and Table 4), analogous to the behavior observed with Gram-negative bacteria (*P. aeruginosa*). Of note, a greater concentration of NO-releasing G2-PPI-PO **1a** was required to completely kill all *S. aureus* cells compared to the control G2-PO-modified dendrimer **1**. These results may be attributed to the decreased interactions between the dendrimer and bacterial membrane resulting from the negative zeta potential of the NO-releasing G2-PPI-PO **1a** ( $-14.0 \pm 5.4$  mV; Table 2).

To confirm whether the lessened antibacterial activity of the NO-releasing G2-PPI-PO **1a** was indeed the result of decreased dendrimer interactions (with the *S. aureus* cell membrane), confocal microscopy was used to compare the association kinetics of NO-releasing G2-PPI-PO **1a** and control PO-modified dendrimer **1** (zeta potential =  $+7.1 \pm 0.6$  mV; Table 2) with the bacteria cells. Rhodamine isothiocyanate (RITC)-labeled control and NO-releasing G2-PPI-PO dendrimers (**1** and **1a**) ( $400 \mu\text{g}\cdot\text{mL}^{-1}$ ) were added to the bacteria cell suspension and images were collected every 2 min. As expected, control dendrimer **1** associated with the *S. aureus* cells rapidly (4 min) while the time required for association of the NO-releasing dendrimer **1a** with the bacteria was greater (12 min; Figure 5). In all experiments, the red fluorescence intensity increased as the degree of association between the dendrimers and bacteria increased. Of note, the fluorescence for the control dendrimer **1** was greater than that for the corresponding NO-releasing dendrimer **1a** even after 45 min, indicating that the NO-releasing dendrimers do not associate as readily. These observations confirm that interactions between the NO-releasing G2-PPI-PO dendrimers and *S. aureus* were less than that of the controls, further corroborating the efficacy observed with the bactericidal assays.

The specific exterior modification was also found to influence the bactericidal efficacy against *S. aureus*, with SO- and PEG-modified dendrimers having the greatest and least effects, respectively, analogous to what we observed with *P. aeruginosa*. As well, NO delivered from G5 dendrimers exhibited greater bactericidal efficacy than that from the smaller (G2) analogues (Table 4), reaffirming that *N*-diazeniumdiolate NO donor density and greater localized NO delivery benefited *S. aureus* killing.

As shown in Tables 3 and 4, the G5 dendrimer concentrations required to kill the Gram-positive bacteria (*S. aureus*) were generally less than that needed to eradicate *P. aeruginosa*. The improved antimicrobial efficacy for G5 dendrimers against Gram-positive over Gram-negative bacteria likely arises from their distinct cell-envelope organization. Gram-negative bacteria have an additional lipid membrane barrier that may reduce the diffusion of macromolecular scaffolds. Chen et al. reported similar results with larger molecular weight dendrimers (e.g., quaternary ammonium-modified PPI conjugates) being less effective at diffusing across extracellular barriers of Gram-negative bacteria (*E. coli*) compared to Gram-positive *S. aureus*.<sup>15</sup> The enhanced efficacy of the dendrimers against the Gram-positive *S. aureus* is in marked contrast to our previous report describing more effective killing of Gram-negative bacteria using a small molecule NO donor (PROLI/NO).<sup>58</sup> Both Gram-negative *P. aeruginosa* and Gram-positive *S. aureus* were susceptible to control primary amine-functionalized PPI dendrimers, corroborating the results reported by others using primary amine-functionalized PAMAM conjugates (PAMAM-NH<sub>2</sub>) as antibacterial agents.<sup>14,17</sup> The inherent biocidal action of primary amine-functionalized controls is the result of both electrostatic (protonated primary amines) and hydrophobic interactions

between dendrimers and the negatively-charged bacteria, leading to increased permeability and disruption of the cytoplasmic membrane.

Gaseous NO and NO generated from small molecule NO donors (e.g., PROLI/NO) have exhibited bactericidal efficacy against methicillin-resistant *S. aureus* (MRSA), indicating the potential of NO to kill antibiotic-resistant pathogens.<sup>36,58</sup> To determine if NO-releasing dendrimers were effective against MRSA, bactericidal assays were carried out using SO-modified dendrimers (selected based on their biocidal activity against standard *S. aureus*). As shown in Figure 6, NO-releasing SO-modified G2 and G5 dendrimers (**5a** and **6a**) proved effective against MRSA at lower dendrimer concentrations than control analogues (3-log killing at 2.5 and 0.25  $\mu\text{M}$  for **5a** and **6a** vs. 5 and 0.5  $\mu\text{M}$  for **5** and **6**, respectively). These results are comparable to those observed for standard *S. aureus*.

Antibacterial therapeutics with maximal bactericidal efficacy are often necessary to circumvent the emergence of bacterial resistance.<sup>59</sup> In this context, we evaluated the ability of NO-releasing dendrimers (e.g., *N*-diazoniumdiolate-modified PPI-SO conjugates) to reduce bacterial viability by 5 orders of magnitude (i.e., 99.999% killing). As shown in Table 5, both G2 and G5 NO-releasing PPI-SO (**5a** and **6a**) exhibited biocidal activity over 5 logs against Gram-negative (*P. aeruginosa*), Gram-positive (*S. aureus*), and the methicillin-resistant (MRSA) pathogen, albeit at concentrations marginally greater than those necessary to achieve 3-log killing. The ability to achieve 99.999% killing further illustrates the potential of NO-releasing dendrimers as highly effective antibacterial therapeutics.

### Cytotoxicity of NO-Releasing Dendrimers against Mammalian Fibroblasts

An inherent toxicity against healthy mammalian cells represents a shortcoming of most dendrimer constructs.<sup>60–65</sup> To determine the influence of size (i.e., generation number or molecular weight) and exterior functionality on the toxicity of NO-releasing dendrimers, the *in vitro* cytotoxicity of both control and NO-releasing dendritic scaffolds was evaluated using a standard MTS cell proliferation assay (L929 mouse fibroblasts).<sup>66</sup> L929 cells are common for *in vitro* cytotoxicity studies due to their prevalence in wound healing and extracellular environments.<sup>61,67,68</sup> A range of concentrations for control and NO-releasing dendrimers was tested to encompass the minimum and twice the minimum concentration of each dendrimer that proved 3-log killing of bacteria against all strains tested. As shown in Figure 7, G5 control dendrimers were found to present significant toxicity to the L929 fibroblasts (e.g., <20% viability) when administered at concentrations necessary to kill bacteria. While both G2-PPI-PO **1** and G2-PPI-NH<sub>2</sub> **7** exhibited minimal toxicity to fibroblast cells at bactericidal concentrations, administering twice the minimum bactericidal concentrations of G2-PEG- and SO-modified dendrimers (**3** and **5**) still inhibited fibroblast proliferation by approximately 76 and 64%, respectively (i.e., 24 and 36% viability). Prior studies have documented generation-dependent toxicity of cationic dendrimers to fibroblasts and other mammalian cell types, clearly indicating that larger dendrimers generally exhibit greater cytotoxicity, consistent with our observations.<sup>61,62,65</sup>

The toxicity of NO-releasing dendrimers **1a–6a** to L929 fibroblasts was minimal (< 60% viability; Figure 8) relative to controls **1–6** (Figure 7) when administered at both the minimum and twice the minimum concentration required to elicit 3-log killing against all tested bacterial strains. Such reduced toxicity is not surprising due to the lower concentrations required for bacteria killing, and may also be attributed to decreased initial cationic charges as evidenced by the less positive zeta potentials for the NO-releasing dendrimers (Table 2). Due to proton-driven dissociation of *N*-diazoniumdiolates to NO, the toxicity of the resulting dendrimer precursors **1–6** (i.e., control dendrimers) to fibroblasts was also evaluated at equivalent doses of their NO-releasing analogues **1a–6a** that proved

bactericidal (Figure 8). These results reveal minimal toxicity for the dendrimer precursors at these concentrations, even though a ~75% reduction in fibroblast viability was observed for the G5-PPI-PEG precursor **4** at the bactericidal concentration of its *N*-diazoniumdiolate-modified derivative **4a** (20  $\mu$ M; Figure 8B). Remarkably, both G2 and G5 NO-releasing PPI-SO dendrimers (**5a** and **6a**) and their precursors (**5** and **6**) proved to be nontoxic to the fibroblast cells (>80 % viability; Figure 8) even at concentrations necessary to induce 5-log killing against all species studied (10 and 1  $\mu$ M, respectively; Table 5). Collectively, these results illustrate the potential of NO-releasing dendrimers as effective scaffolds for combating bacteria with minimal toxicity to healthy mammalian cells.

## Conclusions

The utility of NO-releasing dendrimers as antibacterial therapeutics with broad-spectrum activity was demonstrated through the systematic study of dendrimer size, NO release, and exterior modification. In general, NO-releasing PPI dendrimers exert increased bactericidal activity at concentrations lower than the corresponding antibacterial precursors. The antibacterial efficacy observed across a series of structurally diverse NO-releasing dendritic scaffolds was largely dependent on size and exterior functionality (e.g., hydrophobicity, biocompatibility, etc.). The benefit of NO-releasing dendrimers over quaternary ammonium-functionalized scaffolds was illustrated by their limited toxicity against fibroblasts at concentrations necessary to eradicate bacteria (3-log killing). In particular, G2 and G5 NO-releasing PPI-SO dendrimers proved highly effective (>99.999% killing) against both Gram-positive and Gram-negative bacteria, including the antibiotic-resistant strain, MRSA, while maintaining minimal toxicity against mammalian cells at bactericidal doses. Experiments are underway to examine the possible role of NO-release kinetics on antibacterial efficacy (i.e., short versus extended NO release). Future studies are also planned to exploit the versatility of the exterior modification using multi-NO donor functionalization and specific ligand conjugation strategies (e.g., sugars, antibodies, etc.) that may further enhance the utility of NO-releasing dendritic scaffolds as antibacterial agents.

## Supplementary Material

Refer to Web version on PubMed Central for supplementary material.

## Acknowledgments

Financial support is gratefully acknowledged from the National Institutes of Health (NIH EB000708). The authors thank Dr. Alexis W. Carpenter for preparation of the AHAP3/TEOS particles.

## References

1. Robson MC. *Surg Clin North Am.* 1997; 77:637–650. [PubMed: 9194884]
2. Wright GD. *Nat Rev Microbiol.* 2007; 5:175–186. [PubMed: 17277795]
3. Levy SB, Marshall B. *Nat Med.* 2004; 10:S122–S129. [PubMed: 15577930]
4. Boas U, Heegaard PMH. *Chem Soc Rev.* 2004; 33:43–63. [PubMed: 14737508]
5. Lee CC, MacKay JA, Frechet JMJ, Szoka FC. *Nat Biotechnol.* 2005; 23:1517–1526. [PubMed: 16333296]
6. Mintzer MA, Grinstaff MW. *Chem Soc Rev.* 2011; 40:173–190. [PubMed: 20877875]
7. Debrabandervandenberg EMM, Meijer EW. *Angew Chem, Int Ed.* 1993; 32:1308–1311.
8. Tomalia DA, Naylor AM, Goddard WA. *Angew Chem, Int Ed.* 1990; 29:138–175.
9. Fox ME, Szoka FC, Frechet JMJ. *Acc Chem Res.* 2009; 42:1141–1151. [PubMed: 19555070]
10. Bosman AW, Janssen HM, Meijer EW. *Chem Rev.* 1999; 99:1665–1688. [PubMed: 11849007]
11. Grayson SM, Frechet JMJ. *Chem Rev.* 2001; 101:3819–3867. [PubMed: 11740922]

12. Carlmark A, Hawker CJ, Hult A, Malkoch M. *Chem Soc Rev.* 2009; 38:352–362. [PubMed: 19169453]
13. Patri AK, Kukowska-Latallo JF, Baker JR. *Adv Drug Delivery Rev.* 2005; 57:2203–2214.
14. Calabretta MK, Kumar A, McDermott AM, Cai CZ. *Biomacromolecules.* 2007; 8:1807–1811. [PubMed: 17511499]
15. Chen CZS, Beck-Tan NC, Dhurjati P, van Dyk TK, LaRossa RA, Cooper SL. *Biomacromolecules.* 2000; 1:473–480. [PubMed: 11710139]
16. Meyers SR, Juhn FS, Griset AP, Luman NR, Grinstaff MW. *J Am Chem Soc.* 2008; 130:14444–14445. [PubMed: 18842041]
17. Lopez AI, Reins RY, McDermott AM, Trautner BW, Cai CZ. *Mol Biosyst.* 2009; 5:1148–1156. [PubMed: 19756304]
18. Lee CC, Gillies ER, Fox ME, Guillaudeu SJ, Frechet JMJ, Dy EE, Szoka FC. *Proc Natl Acad Sci USA.* 2006; 103:16649–16654. [PubMed: 17075050]
19. Morgan MT, Carnahan MA, Immoos CE, Ribeiro AA, Finkelstein S, Lee SJ, Grinstaff MW. *J Am Chem Soc.* 2003; 125:15485–15489. [PubMed: 14664594]
20. Morgan MT, Nakanishi Y, Kroll DJ, Griset AP, Carnahan MA, Wathier M, Oberlies NH, Manikumar G, Wani MC, Grinstaff MW. *Cancer Res.* 2006; 66:11913–11921. [PubMed: 17178889]
21. Kukowska-Latallo JF, Candido KA, Cao ZY, Nigavekar SS, Majoros IJ, Thomas TP, Balogh LP, Khan MK, Baker JR. *Cancer Res.* 2005; 65:5317–5324. [PubMed: 15958579]
22. Kukowska-Latallo JF, Bielinska AU, Johnson J, Spindler R, Tomalia DA, Baker JR. *Proc Natl Acad Sci USA.* 1996; 93:4897–4902. [PubMed: 8643500]
23. Haensler J, Szoka FC. *Bioconjugate Chem.* 1993; 4:372–379.
24. Patil ML, Zhang M, Taratula O, Garbuzenko OB, He HX, Minko T. *Biomacromolecules.* 2009; 10:258–266. [PubMed: 19159248]
25. Choi JS, Nam K, Park J, Kim JB, Lee JK, Park J. *J Controlled Release.* 2004; 99:445–456.
26. Taratula O, Garbuzenko OB, Kirkpatrick P, Pandya I, Savla R, Pozharov VP, He HX, Minko T. *J Controlled Release.* 2009; 140:284–293.
27. Luo D, Haverstick K, Belcheva N, Han E, Saltzman WM. *Macromolecules.* 2002; 35:3456–3462.
28. Wathier M, Jung PJ, Carnahan MA, Kim T, Grinstaff MW. *J Am Chem Soc.* 2004; 126:12744–12745. [PubMed: 15469247]
29. Duan XD, McLaughlin C, Griffith M, Sheardown H. *Biomaterials.* 2007; 28:78–88. [PubMed: 16962168]
30. Sontjens SHM, Nettles DL, Carnahan MA, Setton LA, Grinstaff MW. *Biomacromolecules.* 2006; 7:310–316. [PubMed: 16398530]
31. Khew ST, Yang QJ, Tong YW. *Biomaterials.* 2008; 29:3034–3045. [PubMed: 18420267]
32. Chen CZS, Cooper SL. *Adv Mater.* 2000; 12:843–846.
33. Fang FC. *J Clin Invest.* 1997; 99:2818–2825. [PubMed: 9185502]
34. Fang FC. *Nat Rev Microbiol.* 2004; 2:820–832. [PubMed: 15378046]
35. MacMicking J, Xie QW, Nathan C. *Annu Rev Immunol.* 1997; 15:323–350. [PubMed: 9143691]
36. Ghaffari A, Miller CC, McMullin B, Ghahary A. *Nitric Oxide-Biol Chem.* 2006; 14:21–29.
37. Hetrick EM, Schoenfish MH. *Chem Soc Rev.* 2006; 35:780–789. [PubMed: 16936926]
38. Riccio DA, Schoenfish MH. *Chem Soc Rev.* 2012; 41:3731–3741. [PubMed: 22362355]
39. Carpenter AW, Schoenfish MH. *Chem Soc Rev.* 2012; 41:3742–3752. [PubMed: 22362384]
40. Coneski PN, Schoenfish MH. *Chem Soc Rev.* 2012; 41:3753–3758. [PubMed: 22362308]
41. Nichols SP, Storm WL, Koh A, Schoenfish MH. *Adv Drug Deliv Rev.* 2012; 64:1177–1188. [PubMed: 22433782]
42. Polizzi MA, Stasko NA, Schoenfish MH. *Langmuir.* 2007; 23:4938–4943. [PubMed: 17375944]
43. Rothrock AR, Donkers RL, Schoenfish MH. *J Am Chem Soc.* 2005; 127:9362–9363. [PubMed: 15984851]
44. Stasko NA, Schoenfish MH. *J Am Chem Soc.* 2006; 128:8265–8271. [PubMed: 16787091]

45. Stasko NA, Fischer TH, Schoenfish MH. *Biomacromolecules*. 2008; 9:834–841. [PubMed: 18247567]
46. Lu Y, Sun B, Li CH, Schoenfish MH. *Chem Mater*. 2011; 23:4227–4233. [PubMed: 22053127]
47. Shin JH, Metzger SK, Schoenfish MH. *J Am Chem Soc*. 2007; 129:4612–4619. [PubMed: 17375919]
48. Shin JH, Schoenfish MH. *Chem Mater*. 2008; 20:239–249.
49. Riccio DA, Nugent JL, Schoenfish MH. *Chem Mater*. 2011; 23:1727–1735. [PubMed: 21499510]
50. Carpenter AW, Slomberg DL, Rao KS, Schoenfish MH. *Acs Nano*. 2011; 5:7235–7244. [PubMed: 21842899]
51. Carpenter AW, Worley BV, Slomberg DL, Schoenfish MH. *Biomacromolecules*. 2012 in press.
52. Hetrick EM, Shin JH, Stasko NA, Johnson CB, Wespe DA, Holmuhamedov E, Schoenfish MH. *Acs Nano*. 2008; 2:235–246. [PubMed: 19206623]
53. Hetrick EM, Schoenfish MH. *Annu Rev Anal Chem*. 2009; 2:409–433.
54. Breed RS, Dotterrer WD. *J Bacteriol*. 1916; 1:321–331. [PubMed: 16558698]
55. Wink DA, Kasprzak KS, Maragos CM, Elespuru RK, Misra M, Dunams TM, Cebula TA, Koch WH, Andrews AW, Allen JS, Keefer LK. *Science*. 1991; 254:1001–1003. [PubMed: 1948068]
56. Chen CZS, Cooper SL. *Biomaterials*. 2002; 23:3359–3368. [PubMed: 12099278]
57. Lucchini JJ, Corre J, Cremieux A. *Res Microbiol*. 1990; 141:499–510. [PubMed: 1697976]
58. Privett BJ, Deupree SM, Backlund CJ, Rao KS, Johnson CB, Coneski PN, Schoenfish MH. *Mol Pharm*. 2010; 7:2289–2296. [PubMed: 20939612]
59. Stratton CW. *Emerg Infect Dis*. 2003; 9:10–16. [PubMed: 12533275]
60. Duncan R, Izzo L. *Adv Drug Delivery Rev*. 2005; 57:2215–2237.
61. Fischer D, Li YX, Ahlemeyer B, Krieglstein J, Kissel T. *Biomaterials*. 2003; 24:1121–1131. [PubMed: 12527253]
62. Jevprasesphant R, Penny J, Jalal R, Attwood D, McKeown NB, D'Emanuele A. *Int J Pharm*. 2003; 252:263–266. [PubMed: 12550802]
63. Malik N, Wiwattanapatapee R, Klopsch R, Lorenz K, Frey H, Weener JW, Meijer EW, Paulus W, Duncan R. *J Controlled Release*. 2000; 65:133–148.
64. Rittner K, Benavente A, Bompard-Sorlet A, Heitz F, Divita G, Brasseur R, Jacobs E. *Mol Ther*. 2002; 5:104–114. [PubMed: 11829517]
65. Roberts JC, Bhalgat MK, Zera RT. *J Biomed Mater Res*. 1996; 30:53–65. [PubMed: 8788106]
66. Cory AH, Owen TC, Barltrop JA, Cory JG. *Cancer Commun*. 1991; 3:207–212. [PubMed: 1867954]
67. Wong T, McGrath JA, Navsaria H. *Br J Dermatol*. 2007; 156:1149–1155. [PubMed: 17535219]
68. Turner TD, Spyratou O, Schmidt RJ. *J Pharm Pharmacol*. 1989; 41:775–780. [PubMed: 2576047]

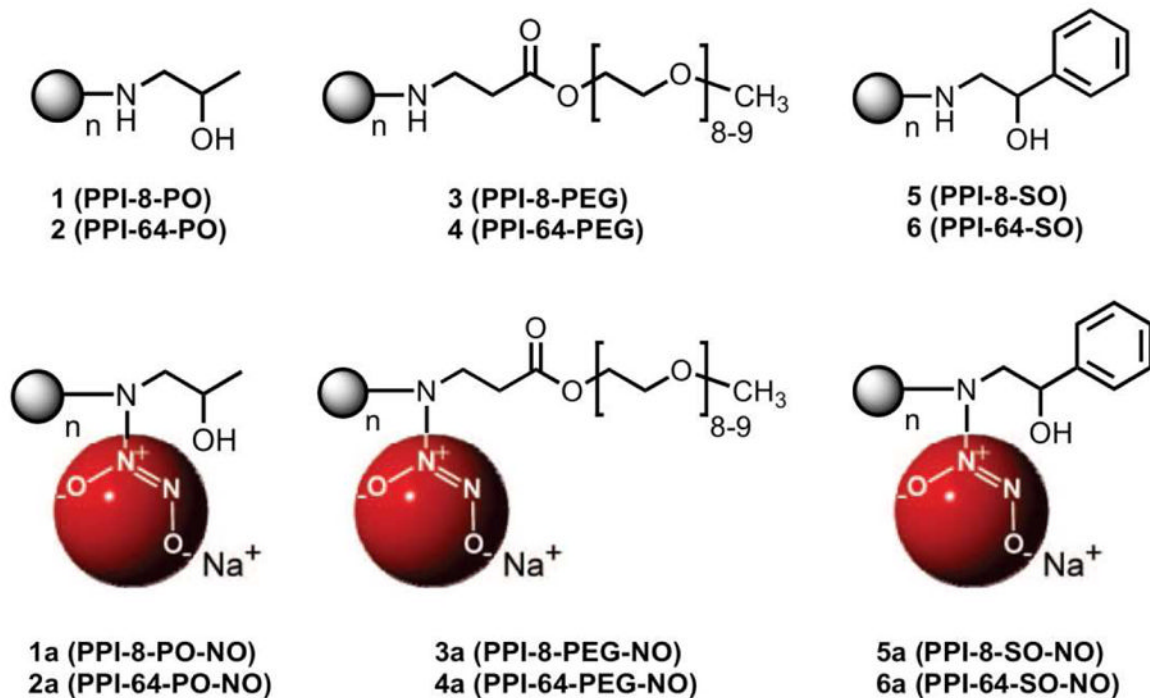


**Figure 1.** Structures of secondary amine- and *N*-diazeniumdiolate NO donor-functionalized G2 (n = 8) and G5 (n = 64) PPI dendrimers.

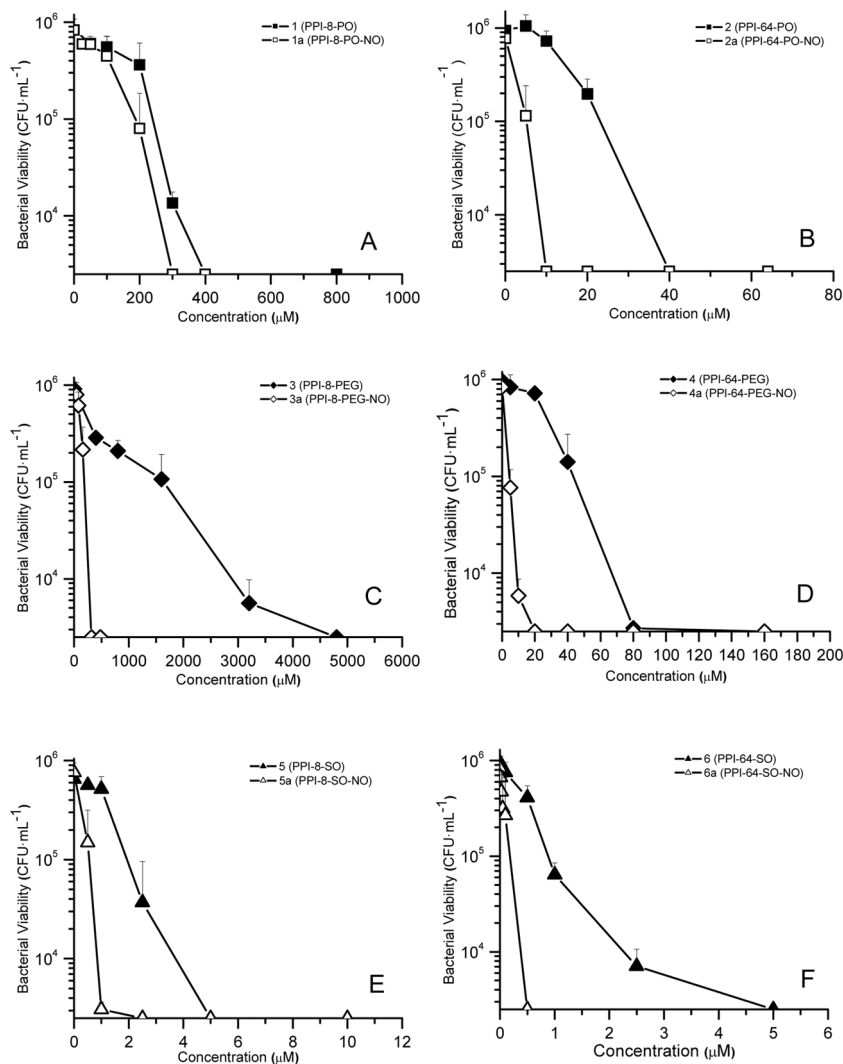


**Figure 2.** Viability of Gram-negative *P. aeruginosa* after 2 h exposure to a range of optimized concentrations of control and NO-releasing PPI dendrimers with (A) G2-PO; (B) G5-PO; (C) G2-PEG; (D) G5-PEG; (E) G2-SO; and, (F) G5-SO modifications.

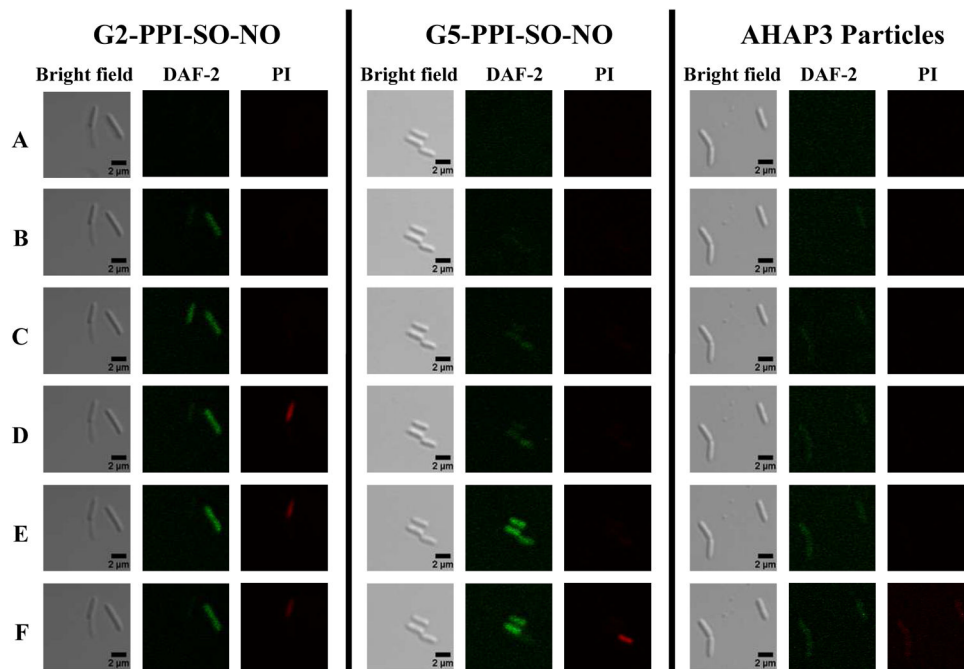


**Figure 3.** Bright field and fluorescent images of *P. aeruginosa* cells exposed to the same NO dosage ( $10 \mu\text{mol}\cdot\text{L}^{-1}$ ) via incubation with NO-releasing G2- and G5-PPI-SO ( $8.7$  and  $10 \mu\text{g}\cdot\text{mL}^{-1}$ , respectively) and  $50 \text{ nm}$  AHAP3/TEOS nanoparticles ( $22 \mu\text{g}\cdot\text{mL}^{-1}$ ). Intracellular NO is indicated by the appearance of DAF-2 green fluorescence, while PI red fluorescence indicates compromised membranes (cell death). Images were acquired (A) 30; (B) 46; (C) 60; (D) 64; (E) 86; and, (F) 94 min after dendrimer/nanoparticle addition.



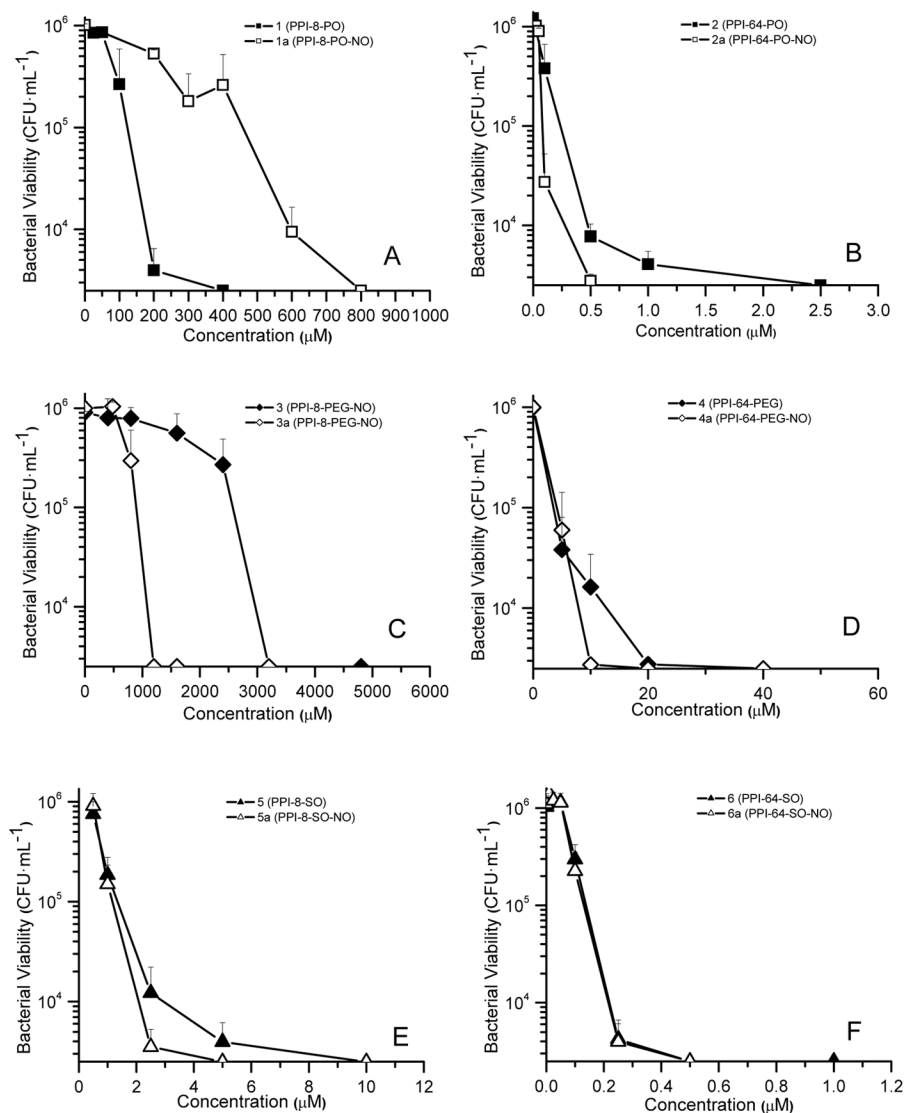


**Figure 4.** Viability of Gram-positive *S. aureus* after 2 h exposure to a range of optimized concentrations of control and NO-releasing PPI dendrimers with (A) G2-PO; (B) G5-PO; (C) G2-PEG; (D) G5-PEG; (E) G2-SO; and, (F) G5-SO modifications.

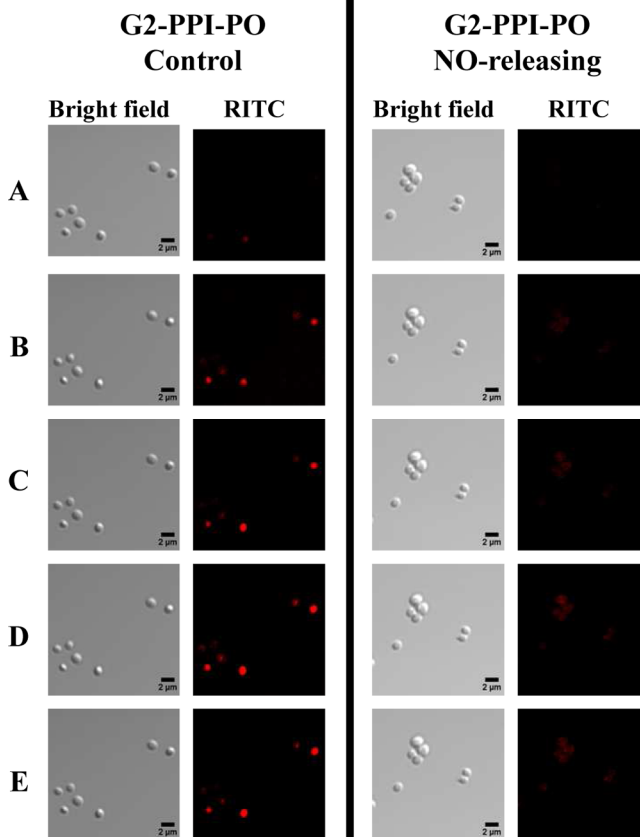


**Figure 5.** Bright field and fluorescent images of RITC-modified control and NO-releasing G2 PPI-PO dendrimer ( $400 \mu\text{g}\cdot\text{mL}^{-1}$ ) association with *S. aureus* cells. Images were acquired (A) 4; (B) 12; (C) 18; (D) 30; and, (E) 45 min following dendrimer addition.

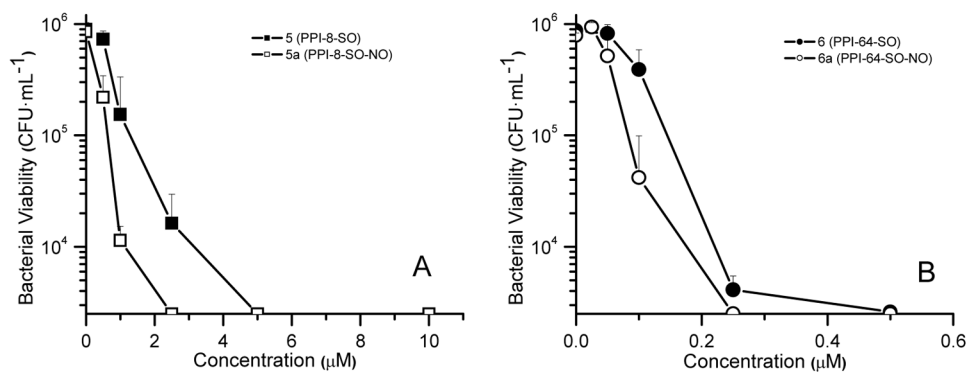


**Figure 6.** Comparison of the bactericidal efficacies of control and NO-releasing (A) G2 and (B) G5 PPI-SO dendrimers against methicillin-resistant *S. aureus* (MRSA) after 2h exposure.

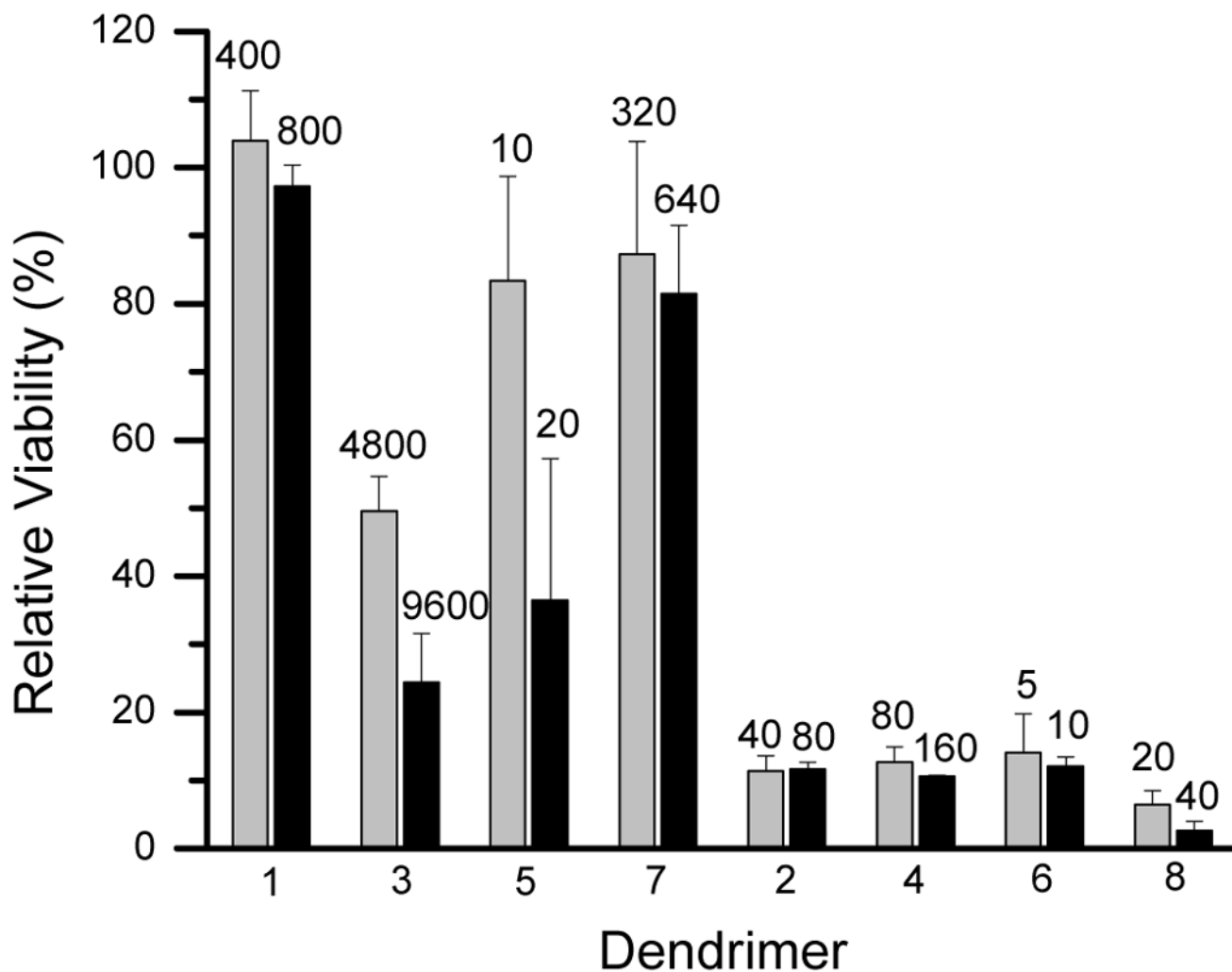


**Figure 7.** Toxicity of G2 (odd number) and G5 (even number) control PPI dendrimers to L929 mouse fibroblasts at both the minimum concentration (light gray) and twice the minimum concentration (black) necessary for 3-log killing against all bacterial strains tested. Dendrimer concentrations are shown above in  $\mu\text{M}$ .

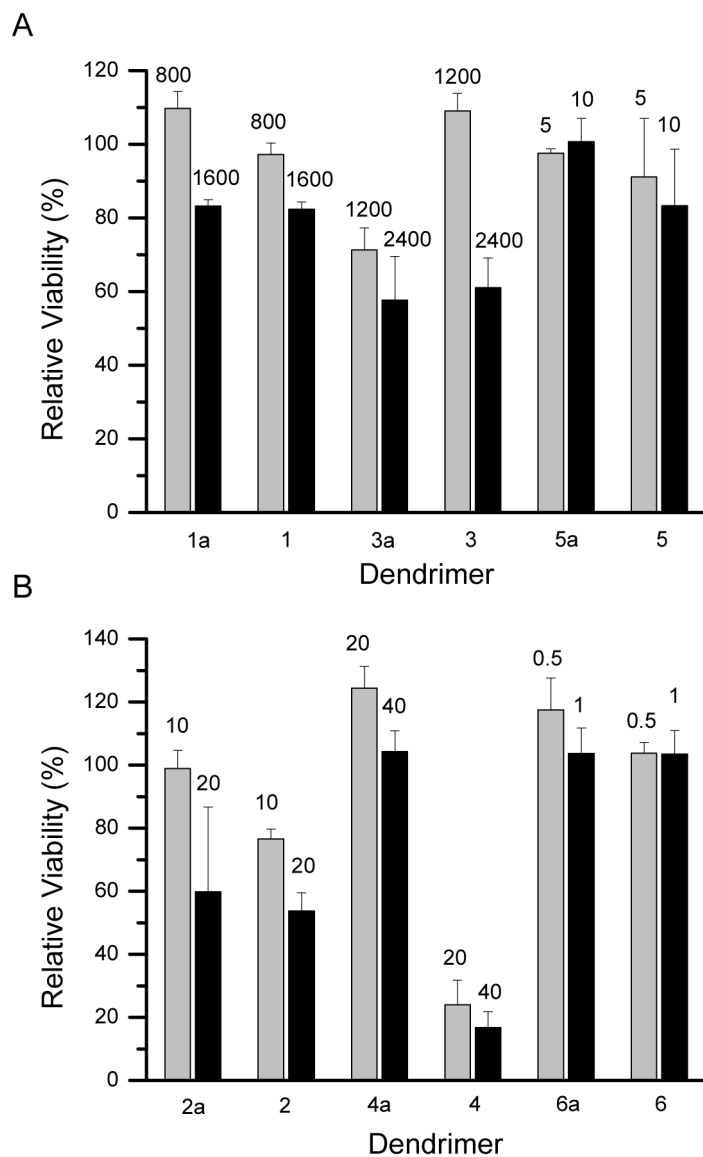


**Figure 8.** Cytotoxicity of (A) G2 and (B) G5 NO-releasing PPI dendrimers **1a–6a** including the corresponding control scaffolds **1–6** (dendrimer precursors) against L929 mouse fibroblasts at the minimum concentration (light gray) and twice the minimum concentration (black) of NO-releasing dendrimers **1a–6a** necessary for 3-log killing against all the bacterial strains tested. Dendrimer concentrations are shown in  $\mu\text{M}$ .

Table 1

Nitric oxide release properties for G2 and G5 PPI dendrimers in PBS (pH = 7.4) at 37 °C

Dendrimer	t[NO] ( $\mu\text{mol}\cdot\text{m g}^{-1}\alpha$ )	t[NO] ( $\mu\text{mol}\cdot\mu\text{mol l}^{-1}\beta$ )	t[NO] <sub>2h</sub> ( $\mu\text{mol}\cdot\text{m g}^{-1}\epsilon$ )	t[NO] <sub>2h</sub> ( $\mu\text{mol}\cdot\mu\text{mol l}^{-1}\delta$ )	[NO] <sub>max</sub> (ppb $\cdot\text{mg}^{-1}\rho$ )	[NO] <sub>max</sub> (ppb $\cdot\mu\text{mol l}^{-1}\gamma$ )	t <sub>m</sub> (min)	t <sub>1/2</sub> (h)	%co nv
1a PPI-8-PO-NO	3.31	4.00	2.47	2.99	9863	11933	1.5	0.84	25.0
2a PPI-64-PO-NO	3.78	41.1	2.61	28.4	6839	74520	2.3	1.06	32.1
3a PPI-8-PEG-NO	1.11	5.10	0.85	3.92	3771	17291	2.1	0.67	31.9
4a PPI-64-PEG-NO	1.17	44.3	0.65	24.6	1886	71403	2.1	1.70	34.6
5a PPI-8-SO-NO	1.77	3.02	1.19	2.02	5241	8943	1.6	1.10	18.9
6a PPI-64-SO-NO	1.84	27.3	1.03	15.2	3178	47128	2.8	1.60	21.3

<sup>a</sup> total NO released and<sup>c</sup> NO released over 2 h ( $\mu\text{mol}$ ) per milligram of secondary amine-functionalized PPI.<sup>b</sup> total NO released and<sup>d</sup> NO released over 2 h ( $\mu\text{mol}$ ) per micromole of secondary amine-functionalized PPI.<sup>e</sup> maximum NO flux (ppb) per milligram of secondary amine-functionalized PPI.<sup>f</sup> maximum NO flux (ppb) per micromole of secondary amine-functionalized PPI.

**Table 2**

Zeta potential of control and NO-releasing dendrimers in phosphate buffer (10 mM, pH = 7.4)

Dendrimer	Zeta Potential ( $\zeta$ ) (mV)
1 PPI-8-PO	7.1±0.6
<b>1a PPI-8-PO-NO</b>	<b>-14.0±5.4</b>
2 PPI-64-PO	11.3±0.3
<b>2a PPI-64-PO-NO</b>	<b>-6.4±0.2</b>
3 PPI-8-PEG	7.1±2.8
<b>3a PPI-8-PEG-NO</b>	<b>-8.5±1.4</b>
4 PPI-64-PEG	8.9±2.6
<b>4a PPI-64-PEG-NO</b>	<b>-4.1±1.3</b>
5 PPI-8-SO	26.2±1.5
<b>5a PPI-8-SO-NO</b>	<b>12.5±1.1</b>
6 PPI-64-SO	20.5±0.6
<b>6a PPI-64-SO-NO</b>	<b>9.3±2.7</b>

**Table 3**

Comparison of the bactericidal efficacy (3-log killing) of control and NO-releasing PPI dendrimers against Gram-negative *P. aeruginosa* after 2 h exposure

Dendrimer	MBC ( $\mu\text{M}$ )	MBC ( $\mu\text{g}\cdot\text{mL}^{-1}$ )	Bactericidal NO Dose ( $\mu\text{mol}\cdot\text{L}^{-1}$ )
1 PPI-8-PO	400	484.0	—
1a PPI-8-PONO	300	242.0	897
<b>2 PPI-64-PO</b>	<b>40</b>	<b>434.3</b>	—
<b>2a PPI-64-PONO</b>	<b>10</b>	<b>108.6</b>	<b>284</b>
3 PPI-8-PEG	4800	22009	—
3a PPI-8-PEG-NO	320	1467.3	1254
<b>4 PPI-64-PEG</b>	<b>80</b>	<b>3029</b>	—
<b>4a PPI-64-PEG-NO</b>	<b>20</b>	<b>757.2</b>	<b>492</b>
5 PPI-8-SO	5	8.5	—
5a PPI-8-SO-NO	1	1.7	2.0
<b>6 PPI-64-SO</b>	<b>5</b>	<b>74.1</b>	—
<b>6a PPI-64-SO-NO</b>	<b>0.5</b>	<b>7.4</b>	<b>7.6</b>
7 PPI-8-NH <sub>2</sub>	320	238.5	—
<b>8 PPI-64-NH<sub>2</sub></b>	<b>20</b>	<b>142.8</b>	—



**Table 4**

Comparison of the bactericidal efficacy (3-log killing) of control and NO-releasing PPI dendrimers against Gram-positive *S. aureus* after 2 h exposure

Dendrimer	MBC ( $\mu\text{M}$ )	MBC ( $\mu\text{g}\cdot\text{mL}^{-1}$ )	Bactericidal NO Dose ( $\mu\text{mol}\cdot\text{L}^{-1}$ )
1 PPI-8-PO	400	484.0	—
1a PPI-8-PO-NO	800	967.9	2392
<b>2 PPI-64-PO</b>	<b>2.5</b>	<b>27.1</b>	—
<b>2a PPI-64-PO-NO</b>	<b>0.5</b>	<b>5.4</b>	<b>14.2</b>
3 PPI-8-PEG	3200	14673	—
3a PPI-8-PEG-NO	1200	5502	4703
<b>4 PPI-64-PEG</b>	<b>20</b>	<b>757.2</b>	—
<b>4a PPI-64-PEG-NO</b>	<b>10</b>	<b>378.6</b>	<b>246</b>
5 PPI-8-SO	10	17.1	—
5a PPI-8-SO-NO	5	8.5	10.1
<b>6 PPI-64-SO</b>	<b>0.5</b>	<b>7.4</b>	—
<b>6a PPI-64-SO-NO</b>	<b>0.5</b>	<b>7.4</b>	<b>7.6</b>
7 PPI-8-NH <sub>2</sub>	320	238.5	—
<b>8 PPI-64-NH<sub>2</sub></b>	<b>2.5</b>	<b>17.8</b>	—

**Table 5**

Minimum bactericidal concentrations and the corresponding NO doses required from NO-releasing PPI-SO dendrimers to elicit a 5-log reduction in bacterial viability ( 99,999% killing)

Species	5a (PPI-8-SO-NO)			6a (PPI-64-SO-NO)		
	MBC ( $\mu\text{M}$ )	MBC ( $\mu\text{g}\cdot\text{mL}^{-1}$ )	Bactericidal NO Dose ( $\mu\text{mol}\cdot\text{L}^{-1}$ )	MBC ( $\mu\text{M}$ )	MBC ( $\mu\text{g}\cdot\text{mL}^{-1}$ )	Bactericidal NO Dose ( $\mu\text{mol}\cdot\text{L}^{-1}$ )
<i>P. aeruginosa</i>	10	17.1	20.2	1	14.8	15.2
<i>S. aureus</i>	10	17.1	20.2	0.5	7.4	7.6
<i>MRSA</i>	10	17.1	20.2	0.5	7.4	7.6